Electronic Supplementary Information

Structure, formation, thermodynamics and interactions in 9-carboxy-10-methylacridinium-based molecular systems

Damian Trzybiński,[a] Beata Zadykowicz,[b] Michał Wera,[b] Illia E. Serdiuk,[b]
Andrzej Sieradzan,[b,c] Artur Sikorski,[b] Piotr Storoniak[b] and Karol Krzymiński[b]

[a] *Faculty of Chemistry, Biological and Chemical Research Centre, University of Warsaw, Żwirki i Wigury 101, 02-089 Warsaw, Poland*
[b] *Faculty of Chemistry, University of Gdańsk, Wita Stwosza Str. 63, 80−308 Gdańsk, Poland*
[c] *Blirt S.A., Trzy Lipy 3/1.38, 80–172 Gdańsk, Poland*

Synthesis and identity of 9-carboxy-10-methylacridinium salts

9-Carboxy-10-methylacridinium chloride (CMACl) and 9-carboxy-10-methylacridinium trifluoromethanesulfonate (CMATfO) were synthesized with high yields (>80%) by adopting published methods[13,S1] and the synthesis steps are presented in Scheme S1. According to that, 9-(chlorocarbonyl)acridine, obtained by the action of excess of thionyl chloride ($SOCl_2$) on acridine-9-carboxylic acid, was stirred at r.t. in excess of anhydrous methanol (c = 60 g L^{-1}) for 2 h. The crude product, after neutralization of the mixture with $NaHCO_3$, was extracted to organic phase (CH_2Cl_2) and purified by column chromatography (stationary phase: SiO_2, mobile phase: cyclohexane/ethyl acetate = 1/1 *v*/*v*), giving bright yellow powder of 9-[(carbonyl)methoxy]acridine (yield: 72%). Analyses: m.p. = 402−403 K (DSC); m/z 238 ($(M+H)^+$) and 261 ($(M+Na)^+$); % element calculated/found for $C_{15}H_{11}NO_2$: C = 75.94/75.58, H = 4.67/4.73, N = 5.90/5.83). The latter ester was heated (3 h, 383−385 K) with 20-fold molar excess of dimethyl sulfate and the product was precipitated with the excess of diethyl ether, yielding yellow powder of 9-[(carbonyl)methoxy]-10-methylacridinium methylsulfate (yield 79%). Analyses: m.p. = 424–425 K (DSC); m/z 252 $(M)^+$ and 193 ($(M-CH_3CO_2)^+$); % element calculated/found for $C_{17}H_{17}NO_6S$: C = 56.19/56.36; H = 4.72/4.89; N = 3.85/3.69; S, 8.82/8.85. The latter compound was dissolved in UP water (c = 105 g L^{-1}), mixed with 10 % solution of NaOH (1/1.1 *v*/*v*) and heated at 393 K for 2 h. The filtrate, after hot filtration, was divided into the two portions and treated with excess of HCl (analytical grade) (for CMACl) or trifluoromethanesulfonic acid (for CMATfO) to assess final pH = 2.0. The resulting salts, precipitated after cooling the reactant mixtures, were separated by filtration, washed with small amount of propan-2-ol and dried in vacuum pistol over P_2O_5 (370–380 K). 9-Carboxy-10-methylacridinium chloride (CMACl) and 9-carboxy-10-methylacridinium trifluoromethanesulfonate (CMATfO) were obtained as deep yellow powders with yields of 81% and 89%, respectively and purity >99%, assessed by RP-HPLC (Figs S1A and S1B). Analyses for CMACl: elemental composition (% found/calculated for $C_{30}H_{23}ClN_2O_4$ (as homoconjugated salt)): C = 70.5/71.8, H = 4.71/4.54, N = 5.47/5.48 (*Vario EL Cube CHNS*, Elementar Analysensysteme GmbH, Germany), m.p. = 510.5–513.0 K (dec.) (*Stuart Melting Point SMP30*, Bibby Scientific Ltd., UK); ^1H NMR (500 MHz, D_2O, 298 K): H1/H8: 8.40 ppm, 2H, d, 8.8 Hz; H4/H5+H3/H6, 8.24 ppm, 4H, m, 7.2–8.8 Hz; H2/H7: 7.84 ppm, t, 8.0 Hz, $>NCH_3$: 4.66 ppm, 3H, s; MALDI-TOF: m/z = 238 (M^+), 239 ($(M+1)^+$), 194 $(CH_3NAcr)^+$. Analysis for CMATfO: elemental composition (% found/calculated for $C_{31}H_{23}F_3N_2O_7S$ (as homoconjugated salt)):

C = 59.2/59.6, H = 3.79/3.71, N = 4.16/4.49, S = 5.48/5.13; m.p. = 506–508 K (dec.); ^{1}H NMR (500 MHz, D_2O, 298 K): H1/H8: 8.33 ppm, 2H, d, 9.3 Hz; H4/H5+H3/H6, 8.16 ppm, 4H, q, 8.5 Hz; H2/H7: 7.84 ppm, t, 7.3 Hz, > NCH_3: 4.65 ppm, 3H, s. MALDI-TOF: m/z = 238 (M^+), 239 ($(M+1)^+$), 194 $(CH_3NAcr)^+$. Differential Scanning Calorimetry experiments (*Netzsch DSC 204* instrument), performed at the temperature ramp of 5 deg min^{-1}, disclosed complex decomposition of CMACl and CMATfO with the endothermic signals centered at 513.0 K and 495.5 K, respectively. Infrared spectra were acquired for CMACl and CMATfO in the range of 4000–2000 cm^{-1} in KBr tablets, using *Bruker IFS66* infrared spectrometer A characteristic H-bonded OH stretching frequency of carboxylic group was observed in all samples in the range of 3420–3340 cm^{-1} and OH deformation vibrations at ca. 2250 and 2800 cm^{-1} (Fig. S1C).

Crystallization of CMACl and CMATfO from H_2O/CH_3CH_2OH mixtures yielded **1**, **2** and **3**. The canonical structures of the investigated crystalline forms, together with the atom labeling scheme are presented in Scheme S2.

[S1] M. M. Rauhut, D. Sheehan, R. A. Clarke, B. G. Roberts and A. M. Semsel, *J. Org. Chem.*, 1965, **30**, 3587.

Scheme S1 The synthesis steps for 9-carboxy-10-methyacridinium chloride (CMACl) and 9-carboxy-10-methyacridinium chloride trifluoromethanesulfonate (CMATfO).

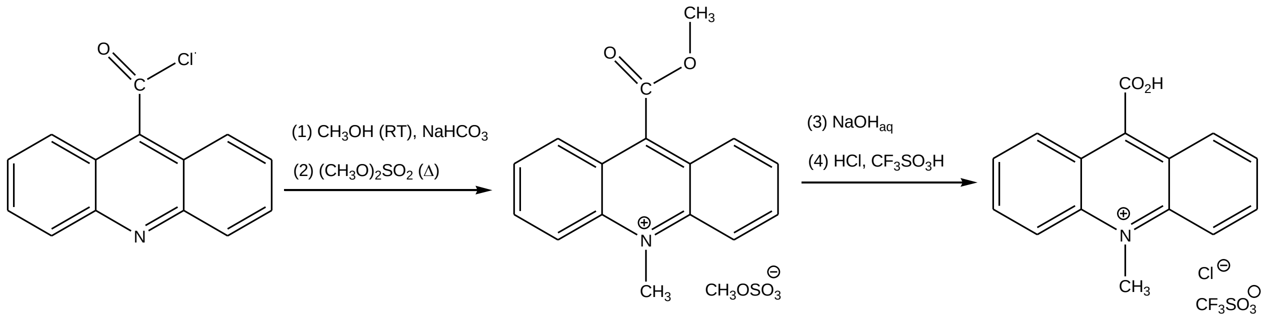

Scheme S2 The canonical structures of investigated acridinium crystalline salts with the atom labeling scheme: 9-carboxy-10-methylacridinium chloride dihydrate (**1**), hydrogen bis(9-carboxy-10-methylacridinium) chloride dihydrate (**2**) and hydrogen bis(9-carboxy-10-methylacridinium) trifluoromethanesulfonate (**3**).

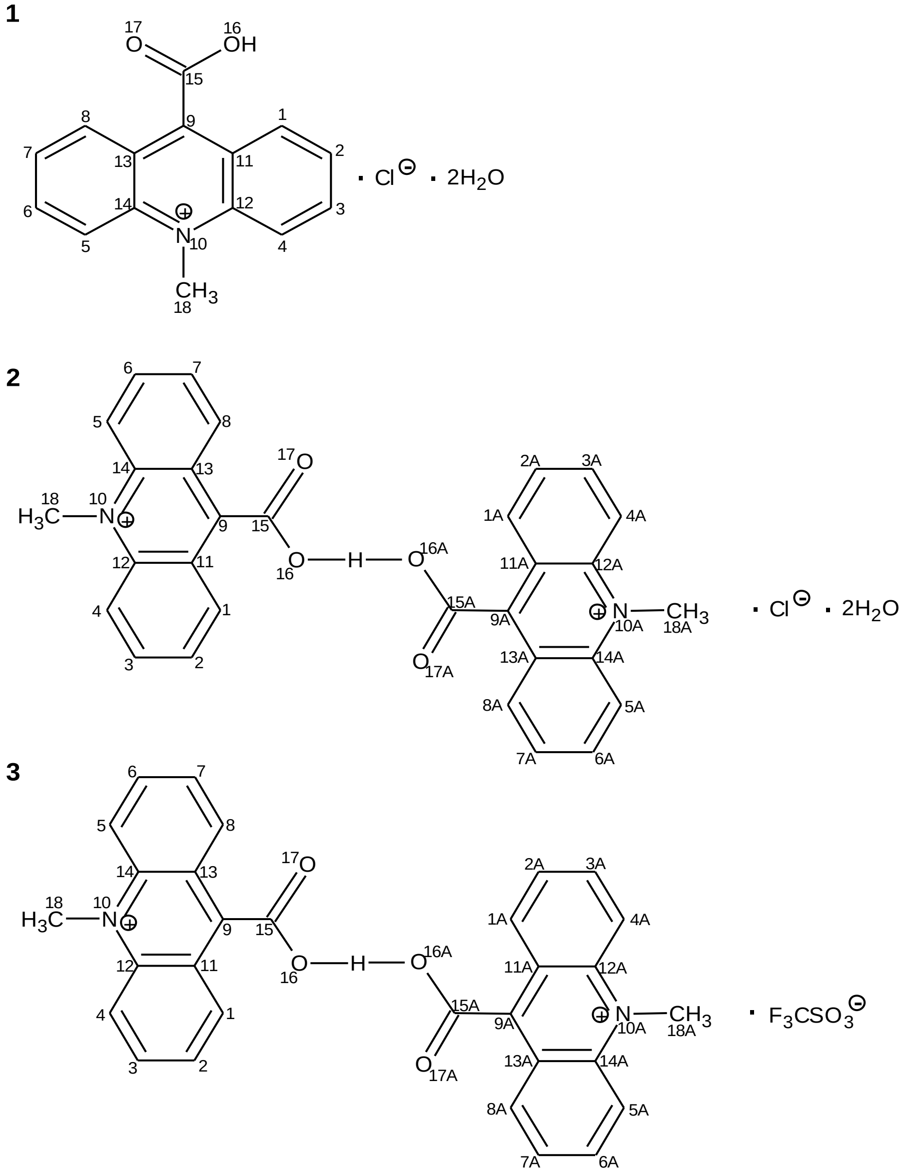

Table S1 Experimental[a] and predicted[b] chemical shifts (in ppm) in NMR spectra of 9-carboxy-10-methylacridinium and hydrogen bis(9-carboxy-10-methylacridinium) cations. **A**: ^{1}H nuclei signals found in compounds **1** and **2** and **3** in various solvents. **B**: ^{13}C nuclei signals found in **1**, **2** and **3** in various solvents (Fig. 1, Scheme S2).

A — **1, 2**

Solvent / No of nuclei[c]	D_2O		DMSO-d_6		CD_3OD		CD_3CN	
	exp	theor	exp	theor	exp	theor	exp	theor
1	8.40	9.70	8.84	9.70	8.71	9.70	8.59	9.70
2	7.84	8.97	8.10	8.97	8.02	8.98	7.88	8.98
3	8.22	9.48	8.38	9.48	8.43	9.48	8.32	9.48
4	8.25	9.55	8.53	9.55	8.54	9.54	8.42	9.55
5	8.25	9.62	8.53	9.62	8.54	9.61	8.42	9.61
6	8.22	9.57	8.38	9.57	8.43	9.57	8.32	9.57
7	7.84	9.04	8.10	9.04	8.02	9.04	7.88	9.04
8	8.40	9.85	8.84	9.85	8.71	9.85	8.59	9.85
16		8.97		8.97		8.96		8.97
		4.92		4.92		4.91		4.92
18	4.66	5.03	4.89	5.03	4.90	5.03	4.70	5.03
		5.20		5.20		5.20		5.20

A — **3**

Solvent / No of nuclei[c,d]	D_2O		DMSO-d_6		CD_3OD		CD_3CN	
	exp	theor	exp	theor	exp	theor	exp	theor
O		22.98		22.98		22.98		22.98
1, 1A	8.41	9.87/9.84	8.83	9.88/9.85	8.73	9.88/9.85	8.54	9.88/9.85
2, 2A	7.85	9.05/9.02	8.08	9.05/9.02	8.04	9.05/9.02	7.96	9.05/9.02
3, 3A	8.23	10.05/10.01	8.37	10.05/10.01	8.45	10.04/10.00	8.38	10.04/10.01
4, 4A	8.26	9.47/9.44	8.52	9.47/9.43	8.54	9.46/9.42	8.52	9.46/9.43
5, 5A	8.26	9.40/9.47	8.52	9.39/9.47	8.54	9.38/9.46	8.52	9.39/9.46
6, 6A	8.23	9.85/9.79	8.37	9.85/9.79	8.45	9.84/9.79	8.38	9.84/9.79
7, 7A	7.85	9.10/9.08	8.08	9.10/9.08	8.04	9.10/9.07	7.96	9.07/9.08
8, 8A	8.41	11.20/11.48	8.83	11.21/11.49	8.73	11.22/11.50	8.54	11.21/11.49
		4.80/4.80		4.79/4.80		4.79/4.79		4.79/4.79
18, 18A	4.68	4.91/4.90	4.88	4.91/4.90	4.92	4.90/4.89	4.72	4.90/4.89
		4.92/4.97		4.91/4.96		4.91/4.96		4.91/4.96

[a] NMR spectra were recorded using Varian Unity 500 Plus spectrometer at room temperature; [b] Method: DFT(B3LYP)/6-31G**– PCM full geometry optimization with inclusion of solvent GIAO; [c] The same as C atom to which H atom is attached (numbering of C atoms is indicated in Fig. 1 and Scheme S2); [d] Nucleus no. O denotes H atom coupling two 9-carboxy-10-methylacridinium moieties in homoconjugated cations (Fig. 1 and Scheme S2).

B — **1, 2**

Solvent / No of nuclei[c]	D_2O		DMSO-d_6
	exp	theor	theor
1, 1A	128.3	134.6	134.6
2, 2A	118.5	131.6	131.6
3, 3A	139.0	147.5	147.5
4, 4A	118.4	118.9	118.8
5, 5A	118.4	119.3	119.2
6, 6A	139.0	147.2	147.2
7, 7A	118.5	131.8	131.7
8, 8A	128.3	133.8	133.8
9, 9A	158.2	159.1	159.1
11, 11A	121.3	126.3	126.3
12, 12A	129.1	143.8	143.8
13, 13A	142.2	126.4	126.3
14, 14A	129.1	144.2	144.1
15, 15A	171.2	167.5	167.4
18, 18A	38.2	30.1	30.0

B — **3**

Solvent / No of nuclei[c]	D_2O		DMSO-d_6
	exp	theor	theor
1, 1A		136.6/138.3	136.7/138.3
2, 2A		130.9/132.5	130.9/132.5
3, 3A		144.9/144.9	144.8/144.9
4, 4A		118.6/118.7	118.5/118.6
5, 5A		120.2/119.7	120.1/119.6
6, 6A		144.6/145.3	144.6/145.3
7, 7A		131.8/131.1	131.7/131.0
8, 8A		138.4/136.4	138.5/136.4
9, 9A		172.0/170.5	172.1/170.5
11, 11A		127.6/124.5	127.6/124.5
12, 12A		145.1/144.2	145.1/144.2
13, 13A		126.2/127.7	126.2/127.7
14, 14A		143.6/145.1	143.5/145.0
15, 15A		169.6/168.2	169.5/168.1
18, 18A		30.5/31.0	30.4/30.9

[a] NMR spectra were recorded on a Varian Unity 500 Plus spectrometer at room temperature; [b] Method: DFT(B3LYP)/6-31G** – PCM full geometry optimization with inclusion of solvent GIAO; [c] Numbering of C atoms is indicated in Fig. 1 and Scheme S2.

Table S2 Positively charged characteristic fragments observed in mass spectra (MALDI-TOF, ESI-QTOF MS) spectra of compounds **1**, **2** and **3** (see also Fig. 7, Tab. S3, Figs S12–S14). Details are given in Experimental section.

cation	m/z value (rounded)	name of fragment
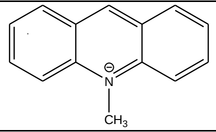	194	10-methylacridinium
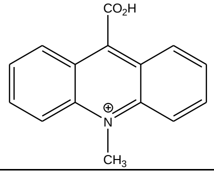	238	9-carboxy- 10-methylacridinium
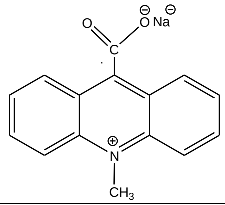	260	9-carboxy- 10-methylacridinium, complex with sodium
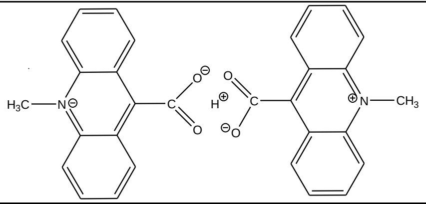	475	homo-conjugated cation
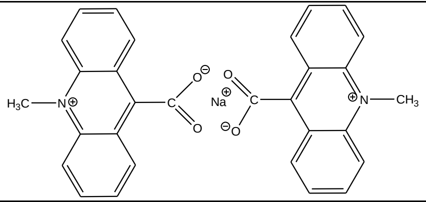	497	homoconjugated cation, complex with sodium
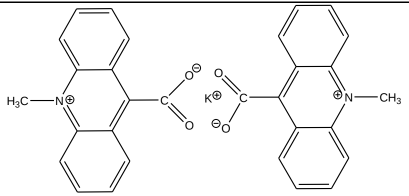	513	homoconjugated cation, complex with potassium

Table S3 Characteristic signals obtained in MALDI-TOF MS spectra recorded for **1**, **2** and **3**. *I* denotes signal intensity (in arbitrary units, a.i.), I_{238}/I_i – the ratio of the moncation signal (I_{238}) to the signal characteristic for of CMA-based homoconjugated cations (I_i). A: in aqueous matrix. B: in anhydrous matrix (acetonitrile; dehydrated samples are denoted as **1dh, 2dh** and **3dh**, respectively). See also Fig. 7 and Table S2 above. Details are given in Experimental section.

Compound No. (Fig. 1, Scheme S2)	**1**		**2**		**3**	
m/z	*I*	I_{238}/I_i	*I*	I_{238}/I_i	*I*	I_{238}/I_i
194	8400	1.0	7600	1.4	6100	0.4
238	**8300**	**1.0**	**11000**	**1.0**	**2600**	**1.0**
475	780	10.6	1050	10.5	550	4.7
497	560	14.8	1350	8.1	3250	0.8
513			150	73.3	400	6.5
	1dh		**2dh**		**3dh**	
194	8880	1.6	8950	1.4	8000	1.4
238	**14000**	**1.0**	**12100**	**1.0**	**11200**	**1.0**
475	1550	9.0	2500	4.8	750	14.9
497	3550	3.9	3200	3.8	1050	10.7
513	350	40.0	200	60.5	150	74.7

Table S4 Calculations of the ionization constant (pK_a), denoting equilibrium between monocationic and homoconjugated forms of **1** in aqueous-ethanolic environment. The Henderson-Hasselbalch method with Haldna correction was employed for calculations of pK_{ai} at various wavelengths (λ). (see also Fig. 8 and Fig. S13). For details see Experimental section.

Experiment No.	λ, nm	pK_{ai}
1	363.1	0.04
2	365.5	0.04
3	367.9	0.04
4	370.4	0.05
5	372.9	0.07
Mean value of pK_a		**0.05**
Std. Dev.		**0.01**
Confidence interval for 95%		**0.01**

Table S5 X-ray diffraction crystal data and structure refinement for compounds **1**, **2** and **3** (Fig. 1).

	1	**2**	**3**
Empirical formula	$C_{15}H_{12}NO_2^{+}\cdot Cl^{-}\cdot 2H_2O$	$C_{30}H_{23}N_2O_4^{+}\cdot Cl^{-}\cdot 2H_2O$	$C_{30}H_{23}N_2O_4^{+}\cdot CF_3SO_3^{-}$
Formula weight	309.74	583.02	624.57
Temperature (K)	295(2)	110(2)	295(2)
Wavelength (Å)	0.71073	0.71073	0.71073
Crystal system	Monoclinic	Monoclinic	Triclinic
Space group	$P2_1/n$	$P2_1/n$	P-1
Unit cell dimensions			
a (Å)	9.2602(6)	9.4378(4)	8.2989(9)
b (Å)	7.3075(4)	7.0489(3)	9.0995(10)
c (Å)	22.2069(12)	21.1972(8)	9.8014(9)
α (º)	90.00	90.00	72.396(9)
β (º)	93.583(5)	97.158(4)	77.357(8)
γ (º)	90.00	90.00	78.795(9)
V ($Å^3$)	1499.78(15)	1399.17(9)	681.82(12)
Z	4	2	1
D_{calcd} (Mg m^{-3})	1.372	1.384	1.521
Abbsorption coefficient (mm^{-1})	0.269	0.289	0.194
Absorption correction type	multi-scan	multi-scan	multi-scan
F(000)	648	612	322
Crystal description	light-orange, prism	light-orange, needle	light-orange, needle
Crystal size (mm)	0.35 x 0.20 x 0.05	0.60 x 0.10 x 0.05	0.50 x 0.15 x 0.05
Θ Range for data collection (º)	3.24 – 25.05	3.48 – 24.99	3.64 – 25.05
Limiting indices	$-11 \le h \le 10$, $-8 \le k \le 7$, $-21 \le l \le 26$	$-11 \le h \le 11$, $-8 \le k \le 8$, $-25 \le l \le 22$	$-9 \le h \le 7$, $-10 \le k \le 10$, $-11 \le l \le 10$
Reflections collected/unique	2644 / 1440	2454 / 2096	2402 / 1562
	[R_{int} = 0.0827]	[R_{int} = 0.0439]	[R_{int} = 0.031]
Completeness 2*Θ* = 25.04º (%)	99.8	99.5	99.7
Refinement method	Full-matrix least-squares on F^2	Full-matrix least-squares on F^2	Full-matrix least-squares on F^2
Data/restraints/parameters	2644 / 6 / 203	2454 / 6 / 204	2408 / 0 / 238
Goodness-of-fit on F^2	0.981	1.107	0.996
Final *R* indices [$I>2\sigma(I)$]	R_1 = 0.0538;	R_1 = 0.0684;	R_1 = 0.0436;
	wR_2 = 0.1196	wR_2 = 0.2128	wR_2 = 0.0909
R indices (all data)	R_1 = 0.1125;	R_1 = 0.0773;	R_1 = 0.0827;
	wR_2 = 0.1512	wR_2 = 0.2259	wR_2 = 0.1072
Extinction coefficient	none	none	0.016(3)
Largest diff. peak and hole (e $Å^{-3}$)	–0.169 and 0.217	–0.335 and 1.163	–0.128 and 0.181
CCDC number	CCDC 981470	CCDC 981472	CCDC 981471

Table S6 Hydrogen-bonding interactions (bond lengths and distances in Å and angles in degrees) in **1**.

D–H···A	D–H	H···A	D···A	D–H···A
O1W–H1W···Cl1	0.86(3)	2.20(3)	3.041(2)	167(3)
O1W–H2W···O2W	0.85(3)	1.83(3)	2.666(4)	166(3)
O2W–H3W···Cl1$^{(i)}$	0.85(2)	2.28(2)	3.133(3)	178(6)
O2W–H4W···Cl1$^{(ii)}$	0.85(3)	2.29(2)	3.121(3)	168(4)
O16–H16···O1W	0.82	1.66	2.471(3)	168

Symmetry codes: (i) = –x + 1/2, y – 1/2, –z + 3/2; (ii) = x, y – 1, z.

Table S7 π–π interactions (distances in Å and angles in degrees) in **1**.

CgI[a]	***CgJ***[a]	***Cg···Cg***[b]	**Dihedral angle**[c]	**Interplanar distance**[d]	**Offset**[e]
1	2$^{(iii)}$	3.753(2)	2.30(14)	3.578(2)	1.133(2)
1	2$^{(iv)}$	3.611(2)	2.30(14)	3.510(2)	0.848(2)
2	1$^{(iii)}$	3.753(2)	2.30(14)	3.618(2)	0.997(2)
2	1$^{(iv)}$	3.611(2)	2.30(14)	3.536(2)	0.732(2)

[a] *Cg* represents the centre of gravity of the rings: *Cg*1, C9/C11/C12/N10/C14/C13; *Cg*2, C1–C4/C12/C11.
Symmetry codes: (iii) –x, –y, –z + 1 ; (iv) –x, –y + 1, –z +1.
[b] *Cg*...*Cg* is the distance between ring centroids.
[c] The dihedral angle is that between the mean planes of *CgI* and *CgJ*.
[d] The interplanar distance is the perpendicular distance of *CgI* from ring *J*.
[e] The offset is the distance between *CgI* and the perpendicular projection of *CgJ* on ring *I*.

Table S8 Hydrogen-bonding interactions (bond lengths and distances in Å and angles in degrees) in **2**.

D–H···A	**D–H**	**H···A**	**D···A**	**D–H···A**
O1W–H1W···O2W(i)	0.81(3)	2.02(4)	2.820(4)	167(3)
O1W–H2W···Cl1	0.82(3)	2.12(3)	2.937(3)	176(6)
O2W–H3W···O17(ii)	0.87(3)	2.29(4)	3.117(4)	160(4)
O2W–H4W···Cl1	0.89(2)	2.30(4)	2.904(4)	125(4)
O16–H16···O16A(iii)	1.22	1.22	2.435(3)	180
C1–H1···Cl1	0.95	2.71	3.560(3)	149
C2–H2···O1W(iv)	0.95	2.60	3.519(4)	163
C18–H18B···Cl1(v)	0.98	2.80	3.735(3)	160

Symmetry codes: (i) = x, y + 1, z; (ii) = –x + 2, –y, –z + 1; (iii) = –x + 2, –y + 1, –z + 1; (iv) = –x + 3/2, y – 1/2, –z + 1/2; (v) = –x + 1, –y + 1, –z + 1.

Table S9 π–π interactions (distances in Å and angles in degrees) in **2**.

CgI[a]	***CgJ***[a]	***Cg···Cg***[b]	**Dihedral angle**[c]	**Interplanar distance**[d]	**Offset**[e]
1	1(v)	3.917(2)	0.0	3.504(2)	1.751(2)
1	2(vi)	3.517(2)	1.90(12)	3.414(2)	0.845(2)
1	2(v)	3.571(2)	1.90(12)	3.472(2)	1.250(2)
2	1(vi)	3.517(2)	1.90(12)	3.436(2)	0.750(2)
2	1(v)	3.571(2)	1.90(12)	3.473(2)	0.831(2)
2	3(v)	3.860(2)	3.06(13)	3.474(2)	1.683(2)
3	2(v)	3.860(2)	3.06(13)	3.398(2)	1.831(2)

[a] *Cg* represents the centre of gravity of the rings: *Cg*1, C9/C11/C12/N10/C14/C13; *Cg*2, C1–C4/C12/C11; *Cg*3, C5–C8/C13/C14.
Symmetry codes: (v) = –x + 1, –y + 1, –z + 1; (vi) = –x + 1, –y, –z + 1.
[b] Cg...Cg is the distance between ring centroids.
[c] The dihedral angle is that between the mean planes of *CgI* and *CgJ*.
[d] The interplanar distance is the perpendicular distance of *CgI* to from *J*.
[e] The offset is the distance between *CgI* and the perependicular projection of *CgJ* on ring *I*.

Table S10 O···Cl interactions (distances in Å) in **2**.

D	**A**	**D···A**
O2W	Cl1$^{(vii)}$	2.904(4)
O1W	O1W$^{(iv)}$	2.994(3)

Symmetry code: (iv) = –x + 3/2, y + 1/2, –z + 1/2.

Table S11 Hydrogen-bonding interactions (bond lengths and distances in Å and angles in degrees) in **3**.

D–H···A	**D–H**	**H···A**	**D···A**	**D–H···A**
O16–H16···O16A$^{(i)}$	1.22	1.22	2.449(2)	180
C1–H1···O21	0.93	2.58	3.360(2)	142
C18–H18A···O17$^{(ii)}$	0.96	2.54	3.199(3)	126
C18–H18B···O21$^{(ii)}$	0.96	2.55	3.370(3)	143

Symmetry codes: (i) –x + 2, –y + 2, –z; (ii) x, y – 1, z.

Table S12 π–π interactions (distances in Å and angles in degrees) in **3**.

CgI[a]	***CgJ***[a]	***Cg···Cg***[b]	**Dihedral angle**[c]	**Interplanar distance**[d]	**Offset**[e]
1	1$^{(iii)}$	3.980(2)	0.0	3.625(1)	1.643(2)
1	3$^{(iii)}$	3.764(2)	2.67(10)	3.584(1)	1.150(2)
2	2$^{(iv)}$	3.692(2)	0.0	3.537(2)	1.059(2)
2	3$^{(iii)}$	3.880(2)	5.23(11)	3.429(2)	1.815(2)
3	1$^{(iii)}$	3.764(2)	2.67(10)	3.567(1)	1.202(2)
3	2$^{(iii)}$	3.880(2)	5.23(11)	3.580(1)	1.496(2)
3	3$^{(v)}$	4.068(2)	0.0	3.429(1)	2.188(2)

[a] *Cg* represents the centre of gravity of the rings: *Cg*1, C9/C11/C12/N10/C14/C13; *Cg*2, C1–C4/C12/C11; *Cg*3, C5–C8/C13/C14.
Symmetry codes: (iii) = –x + 2, –y + 1, –z; (iv) = –x + 2, –y + 1, –z + 1; (v) = –x + 3, –y + 1, –z.
[b] *Cg*...*Cg* is the distance between ring centroids.
[c] The dihedral angle is that between the mean planes of *CgI* and *CgJ*.
[d] The interplanar distance is the perpendicular distance of *CgI* from ring *J*.
[e] The offset is the distance between *CgI* and the perpendicular projection of *CgJ* on ring *I*.

Table S13 Structural parameters of compounds **1**, **2** and **3** (Fig. 1) in crystalline solid phase determined experimentally (X-ray crystallography of monocrystals) and the parameters of constituting them cations in gaseous phase obtained computationally (DFT/6-31G** level). For details see Experimental section.

Compound (Scheme S2)	**1**		**2**		**3**	
Methods	X-ray	DFT	X-ray	DFT	X-ray	DFT
			Bond lengths [Å]			
C1–C2/C1A–C2A	1.343(5)	1.386	1.357(4)	1.373/1.375	1.350(3)	1.369/1.374
C1–C11/C1A–C11A	1.424(4)	1.419	1.425(4)	1.425/1.426	1.423(3)	1.430/1.422
C2–C3/C2A–C3A	1.393(5)	1.379	1.417(4)	1.411/1.410	1.404(3)	1.415/1.411
C3–C4/C3A–C4A	1.367(5)	1.395	1.368(4)	1.379/1.384	1.350(3)	1.376/1.381
C4–C12/C4A–C12A	1.418(4)	1.404	1.416(4)	1.417/1.411	1.416(3)	1.417/1.416
C5–C6/C5A–C6A	1.352(5)	1.395	1.368(4)	1.385/1.380	1.345(3)	1.377/1.384
C5–C14/C5A–C14A	1.418(4)	1.403	1.416(4)	1.410/1.417	1.412(3)	1.420/1.414
C6–C7/C6A–C7A	1.389(5)	1.397	1.412(4)	1.411/1.411	1.405(3)	1.415/1.413
C7–C8/C7A–C8A	1.364(5)	1.386	1.357(4)	1.370/1.374	1.346(3)	1.370/1.372
C8–C13/C8A–C13A	1.427(4)	1.420	1.422(4)	1.428/1.424	1.428(3)	1.426/1.425
C9–C11/C9A–C11A	1.393(4)	1.430	1.393(4)	1.416/1.411	1.398(3)	1.403/1.414
C9–C13/C9A–C13A	1.400(4)	1.436	1.399(4)	1.404/1.417	1.393(3)	1.405/1.410
C9–C15/C9A–C15A	1.515(5)	1.499	1.517(3)	1.523/1.527	1.517(3)	1.519/1.523
N10–C12/N10A–C12A	1.374(4)	1.399	1.369(3)	1.379/1.387	1.368(2)	1.377/1.383
N10–C14/N10A–C14A	1.370(4)	1.406	1.374(3)	1.385/1.381	1.373(2)	1.374/1.387
N10–C18/N10A–C18A	1.479(4)	1.454	1.480(3)	1.470/1.469	1.485(2)	1.479/1.469
C11–C12/C11A–C12A	1.419(4)	1.432	1.433(4)	1.432/1.436	1.420(2)	1.440/1.430
C13–C14/C13A–C14A	1.417(4)	1.431	1.427(4)	1.441/1.431	1.428(2)	1.433/1.433
C15–O17/C15A–O17A	1.199(4)	1.241	1.209(3)	1.217/1.236	1.208(2)	1.212/1.239
C15–O16/C15A–O16A	1.288(4)	1.303	1.278(3)	1.306/1.269	1.265(2)	1.318/1.265
S19–O20					1.435(17)	1.477
S19–O22					1.45(3)	1.490
S19–O21					1.46(2)	1.486
S19–C23					1.772(16)	1.862
C23–F25					1.27(3)	1.342
C23–F24					1.33(2)	1.353
C23–F26					1.39(3)	1.340
			Valence angles [º]			
C2–C1–C11/C2A–C1A–C11A	120.6(3)	122.0	121.3(2)	121.2/121.1	121.0(2)	120.3/121.0
C1–C2–C3/C1A–C2A–C3A	120.5(4)	119.9	119.1(2)	119.5/119.0	119.6(2)	119.8/119.3
C4–C3–C2/C4A–C3A–C2A	121.8(4)	119.8	121.9(2)	121.3/122.0	121.7(2)	121.9/121.6
C3–C4–C12/C3A–C4A–C12A	119.1(3)	121.0	120.1(2)	120.3/119.9	120.3(2)	119.9/120.2
C6–C5–C14/C6A–C5A–C14A	119.8(3)	120.7	119.7(2)	119.8/120.2	120.1(2)	120.2/120.1
C5–C6–C7/C5A–C6A–C7A	122.5(3)	120.0	121.7(3)	121.6/121.4	121.8(2)	121.6/121.6
C8–C7–C6/C8A–C7A–C6A	120.1(3)	120.0	119.7(3)	119.7/119.4	120.1(2)	119.4/119.1
C7–C8–C13/C7A–C8A–C13A	119.5(3)	121.6	120.7(3)	120.8/121.1	120.7(2)	120.9/121.3
C13–C9–C11/C13A–C9A–C11A	120.8(3)	119.9	120.7(2)	120.0/119.4	120.2(2)	120.2/119.3
C13–C9–C15/C13A–C9A–C15A	119.4(3)	120.2	119.4(2)	119.3/120.3	120.5(2)	120.7/118.8
C11–C9–C15/C11A–C9A–C15A	119.8(3)	119.9	119.9(2)	120.7/120.3	119.3(2)	119.1/121.8
C12–N10–C14/C12A–N10A–C14A	121.4(3)	121.7	121.5(2)	121.8/121.5	121.9(2)	121.6/121.5
C12–N10–C18/C12A–N10A–C18A	117.9(3)	119.2	121.0(2)	119.4/119.0	118.1(2)	120.1/119.5
C14–N10–C18/C14A–N10A–C18A	120.7(3)	119.1	117.5(2)	118.8/119.5	120.(2)	118.2/119.0
C9–C11–C12/C9A–C11A–C12A	119.0(3)	119.6	119.2(2)	119.4/119.5	119.1(2)	119.3/119.7
C9–C11–C1/C9A–C11A–C1A	122.3(3)	123.0	121.7(2)	121.8/121.4	122.1(2)	121.2/120.9
C12–C11–C1/C12A–C11A–C1A	118.7(3)	117.3	119.1(2)	118.8/119.0	118.8(2)	119.5/119.4
N10–C12–C4/N10A–C12A–C4A	120.9(3)	121.1	122.0(2)	121.5/121.5	121.6(2)	121.9/121.9
N10–C12–C11/N10A–C12A–C11A	119.9(3)	119.1	119.6(2)	119.5/119.5	119.9(2)	119.5/119.5
C4–C12–C11/C4A–C12A–C11A	119.2(3)	119.8	118.4(2)	118.9/118.9	118.5(2)	118.6/118.6
C9–C13–C14/C9A–C13A–C14A	118.8(3)	119.2	118.7(2)	119.4/119.8	119.7(2)	119.1/119.9
C9–C13–C8/C9A–C13A–C8A	121.4(3)	123.2	122.0(2)	121.7/121.2	121.9(2)	121.6/121.1
C14–C13–C8/C14A–C13A–C8A	119.8(3)	117.6	119.3(2)	118.8/119.0	118.4(2)	119.3/119.0
N10–C14–C5/N10A–C14A–C5A	121.6(3)	120.8	121.0(2)	121.7/121.7	122.1(2)	121.5/122.0
N10–C14–C13/N10A–C14A–C13A	120.1(3)	119.3	120.1(2)	119.2/119.5	119.0(2)	120.0/119.2
C5–C14–C13/C5A–C14A–C13A	118.3(3)	119.9	118.8(2)	119.1/118.8	118.9(2)	118.5/118.8
O17–C15–O16/O17A–C15A–O16A	126.2(3)	125.4	127.6(2)	128.7/130.9	127.7(2)	128.6/130.6
O17–C15–C9/O17A–C15A–C9A	121.4(3)	120.6	119.0(2)	118.3/114.6	118.5(2)	121.7/113.0
O16–C15–C9/O16A–C15A–C9A	112.4(3)	113.9	113.4(2)	113.0/114.5	113.8(2)	109.8/116.4
O20–S19–O22					105.7(12)	115.0
O20–S19–O21					114.2(10)	115.9
O22–S19–O21					114.2(10)	113.7
O20–S19–C23					115.8(9)	104.3
O22–S19–C23					99.9(13)	102.6

O21–S19–C23					106.4(13)	103.0
F25–C23–F24					112.5(18)	107.7
F25–C23–F26					104.4(17)	108.3
F24–C23–F26					114(2)	107.8
F25–C23–S19					114.2(17)	111.1
F24–C23–S19					102.2(13)	110.3
F26–C23–S19					110.3(14)	111.4

Torsion angles [º]

C11–C1–C2–C3/C11A–C1A–C2A–C3A	1.2(6)	0.7	–0.3(4)	–0.7/1.1	–0.2(3)	0.6/0.5
C1–C2–C3–C4/C1A–C2A–C3A–C4A	–1.5(6)	–1.4	1.6(4)	0.7/–1.3	1.1(4)	0.2/–0.6
C2–C3–C4–C12/C2A–C3A–C4A–C12A	0.8(6)	–0.4	–0.6(4)	0.2/–0.2	–0.9(3)	–0.5/–0.1
C14–C5–C6–C7/C14A–C5A–C6A–C7A	–0.1(5)	0.0	–0.3(4)	1.9/0.3	1.1(3)	0.3/1.3
C5–C6–C7–C8/C5A–C6A–C7A–C8A	2.0(5)	2.3	0.1(5)	–2.6/0.6	–0.2(3)	–0.9/–0.7
C6–C7–C8–C13/C6A–C7A–C8A–C13A	–1.2(5)	0.8	0.2(5)	–0.1/–0.7	–0.2(3)	0.0/–0.6
C13–C9–C11–C12/C13A–C9A–C11A–C12A	1.8(4)	–1.4	–3.3(3)	3.8/–4.5	2.4(3)	4.5/–6.2
C15–C9–C11–C12/C15A–C9A–C11A–C12A	–178.8(3)	–179.6	174.0(2)	–173.7/173.4	–176.1(2)	–174.9/170.3
C13–C9–C11–C1/C13A–C9A–C11A–C1A	–179.7(3)	176.2	176.3(2)	–176.9/175.7	–176.8(2)	–177.5/173.2
C15–C9–C11–C1/C15A–C9A–C11A–C1A	–0.3(4)	–1.9	–6.5(4)	5.5/–6.5	4.7(3)	3.2/–10.3
C2–C1–C11–C9/C2A–C1A–C11A–C9A	–178.8(3)	–175.9	178.7(2)	–179.5/–179.6	178.3(2)	–179.1/–179.0
C2–C1–C11–C12/C2A–C1A–C11A–C12A	–0.2(5)	1.7	–1.8(4)	–0.2/0.6	–0.9(3)	–1.1/0.5
C14–N10–C12–C4/C14A–N10A–C12A–C4A	–177.6(3)	–167.6	–179.0(2)	172.7/–171.9	175.6(2)	176.0/–171.0
C18–N10–C12–C4/C18A–N10A–C12A–C4A	3.0(4)	14.4	0.4(3)	–7.4/9.1	–5.8(3)	–6.6/9.6
C14–N10–C12–C11/C14A–N10A–C12A–C11A	2.0(4)	12.8	2.0(3)	–6.5/8.6	–4.4(3)	–4.0/9.0
C18–N10–C12–C11/C18A–N10A–C12A–C11A	–177.4(3)	–165.2	–178.6(2)	173.4/–170.4	174.2(2)	173.3/170.4
C3–C4–C12–N10/C3A–C4A–C12A–N10A	179.8(3)	–176.7	179.5(2)	179.7/–177.6	179.7(2)	179.9/–178.9
C3–C4–C12–C11/C3A–C4A–C12A–C11A	0.2(5)	2.8	–1.5(4)	–1.1/1.9	–0.3(3)	–0.1/1.1
C9–C11–C12–N10/C9A–C11A–C12A–N10A	–1.5(4)	–6.1	1.3(3)	–0.4/–2.4	2.0(3)	–1.0/–1.8
C1–C11–C12–N10/C1A–C11A–C12A–N10A	179.9(3)	176.1	–178.3(2)	179.6/177.4	–178.8(2)	–179.1/178.8
C9–C11–C12–C4/C9A–C11A–C12A–C4A	178.1(3)	174.3	–177.8(2)	–179.7/178.1	–178.1(2)	178.9/178.2
C1–C11–C12–C4/C1A–C11A–C12A–C4A	–0.5(4)	–3.4	2.7(3)	1.1/–2.1	1.1(3)	0.8/–1.2
C11–C9–C13–C14/C11A–C9A–C13A–C14A	–2.4(4)	2.5	2.1(4)	–0.7/5.4	–4.4(3)	–3.0/7.3
C15–C9–C13–C14/C15A–C9A–C13A–C14A	178.2(3)	–179.3	–175.2(2)	176.9/–172.4	174.1(2)	176.3/169.3
C11–C9–C13–C8/C11A–C9A–C13A–C8A	178.1(3)	–179.6	–177.7(2)	176.4/–174.6	175.7(2)	177.0/–173.4
C15–C9–C13–C8/C15A–C9A–C13A–C8A	–1.3(4)	–1.5	5.1(4)	–6.0/7.5	–5.8(3)	–3.7/9.9
C7–C8–C13–C9/C7A–C8A–C13A–C9A	178.1(3)	179.2	179.5(3)	–173.9/180.0	179.5(2)	–178.6/–178.1
C7–C8–C13–C14/C7A–C8A–C13A–C14A	–1.4(4)	–2.9	–0.3(4)	3.2/–0.1	–0.4(3)	1.4/1.2
C12–N10–C14–C5/C12A–N10A–C14A–C5A	176.4(3)	168.9	177.5(2)	–169.6/171.9	–176.9(2)	–174.5/173.0
C18–N10–C14–C5/C18A–N10A–C14A–C5A	–4.2(4)	–13.1	–1.9(4)	10.5/–9.1	4.5(3)	8.1/–7.6
C12–N10–C14–C13/C12A–N10A–C14A–C13A	–2.6(4)	–11.7	–3.2(4)	9.7/–7.7	2.4(3)	5.5/–7.9
C18–N10–C14–C13/C18A–N10A–C14A–C13A	176.7(3)	166.3	177.4(2)	170.2/171.3	–176.2(2)	–171.9/171.5
C6–C5–C14–N10/C6A–C5A–C14A–N10A	178.4(3)	175.5	179.3(3)	–179.4/179.3	177.7(2)	–178.9/178.4
C6–C5–C14–C13/C6A–C5A–C14A–C13A	–2.5(4)	–3.8	0.1(4)	1.3/–1.1	–1.6(3)	1.0/–0.7
C9–C13–C14–N10/C9A–C13A–C14A–N10A	2.8(4)	3.8	1.2(4)	–6.0/0.6	2.0(3)	–2.0/–0.4
C8–C13–C14–N10/C8A–C13A–C14A–N10A	–177.6(2)	–174.2	–179.1(2)	176.8/–179.4	–178.0(2)	178.1/–179.7
C9–C13–C14–C5/C9A–C13A–C14A–C5A	–176.3(3)	–176.8	–179.6(2)	173.4/–179.1	–178.7(2)	178.1/178.7
C8–C13–C14–C5/C8A–C13A–C14A–C5A	3.2(4)	5.2	0.2(4)	–3.8/1.0	1.3(3)	–1.9/–0.5
C13–C9–C15–O17/C13A–C9A–C15A–O17A	89.9(4)	131.0	93.6(3)	–62.5/109.4	–88.2(2)	102.3/77.1
C11–C9–C15–O17/C11A–C9A–C15A–O17A	–89.5(4)	–50.9	–83.7(3)	115.1/–68.4	90.3(2)	–78.4/–99.5
C13–C9–C15–O16/C13A–C9A–C15A–O16A	–89.9(3)	–50.0	–86.6(3)	118.9/–69.5	92.5(2)	–78.6/–100.2
C11–C9–C15–O16/C11A–C9A–C15A–O16A	90.7(3)	128.2	96.1(3)	–63.6/112.7	–89.0(2)	100.7/83.2
O20–S19–C23–F25					52.5(16)	–58.0
O22–S19–C23–F25					–60.4(16)	62.1
O21–S19–C23–F25					–179.4(16)	–179.5
O20–S19–C23–F24					174.2(16)	–177.4
O22–S19–C23–F24					61.3(16)	–57.3
O21–S19–C23–F24					–57.7(14)	61.1
O20–S19–C23–F26					-64.7(18)	62.9
O22–S19–C23–F26					–178.0(2)	–177.0
O21–S19–C23–F26					63.4(17)	–58.6

Table S14 Thermodynamic data for the monomeric (**1a**–**1c**) and homoconjugated (**2a**–**2e** and **3a**–**3c**) 9-carboxy-10-methlylacridinium (CMA)-based forms in the gaseous phase (see also Table 2 and Fig. S16).

Molecular complex (conformer)	$\boldsymbol{H}_{\mathrm{T}}$[a]	$\boldsymbol{G}_{\mathrm{T}}$[a]
1a	–1396.919417	–1396.993627
1b	–1396.808119	–1396.882469
1c	–1396.808019	–1396.883764
2a	–2180.026718	–2180.138595
2b	–2180.037144	–2180.149977
2c	–2027.203073	–2027.303998
2d	–2027.204083	–2027.303667
2e	–2487.524311	–2487.631041
3a	–2528.403257	–2528.519438
3b	–2528.398114	–2528.517341
3c	–3489.919642	–3490.062429

[a] DFT (B3LYP)/6-31G** thermal enthalpies (H_{T}) and Gibbs' free energies (G_{T}) (gaseous phase, 298.15 K, standard pressure), in Hartree, corresponding to optimized structures in stationary states.

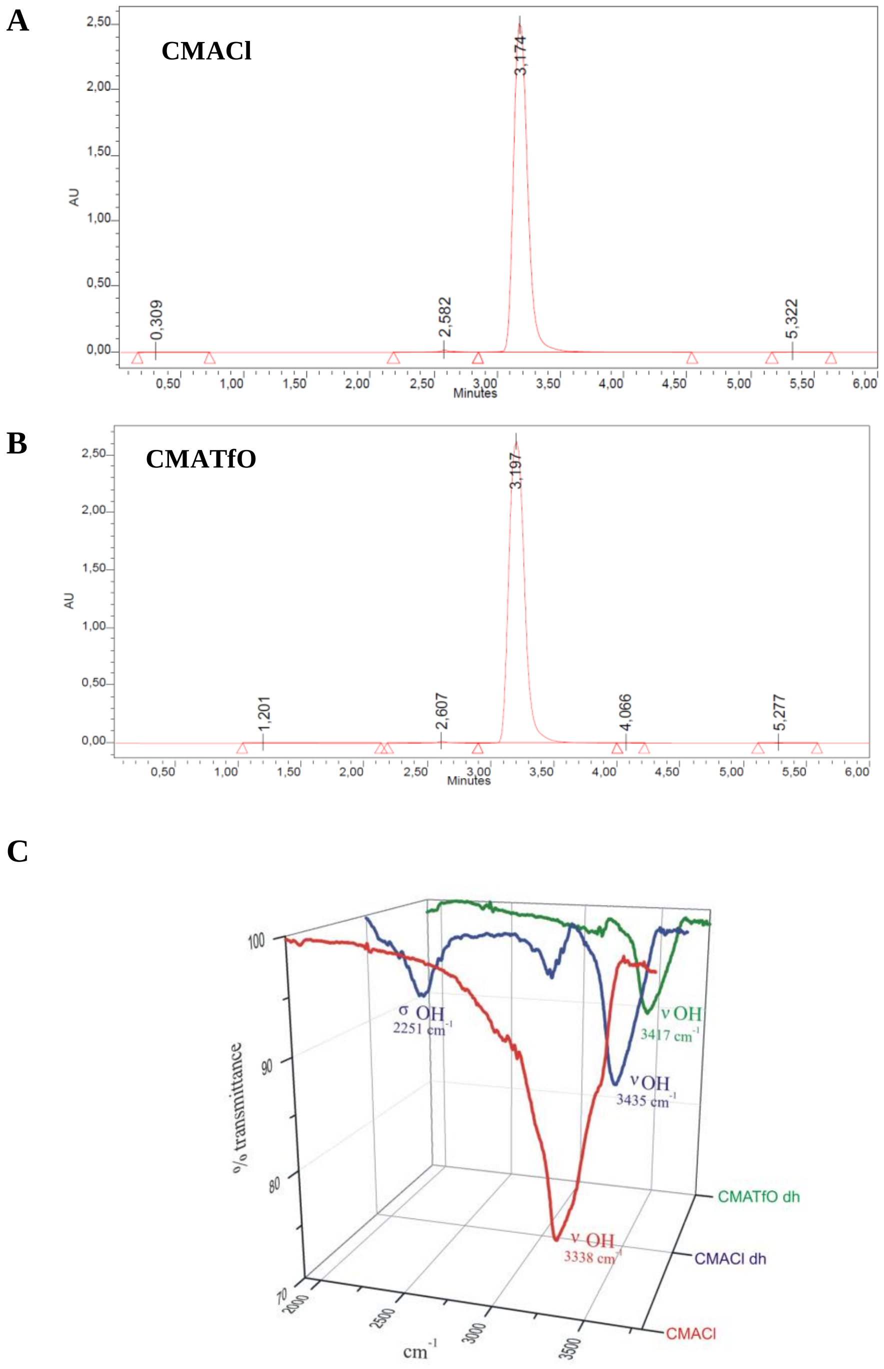

Fig. S1 A, B: RP-HPLC chromatograms for 9-carboxy-10-methylacridinium chloride (CMACl) and 9-carboxy-10-methylacridinium trifluoromethanesulfonate (CMATfO) recorded at 254 nm applying isocratic elution mode (mobile phase: 50% H_2O / 50% acetonitrile, containing 0.05 % trifluoroacetic acid (TFA); stationary phase: Gemini 5µ C6-Phenyl 110 A, *Phenomenex*, USA).

C: The infrared (IR) spectra of CMACl and CMATfO recorded in KBr tablets (dh denotes dried samples). For details see the above text ("Synthesis and identity of 9-carboxy-10-methylacridinium salts").

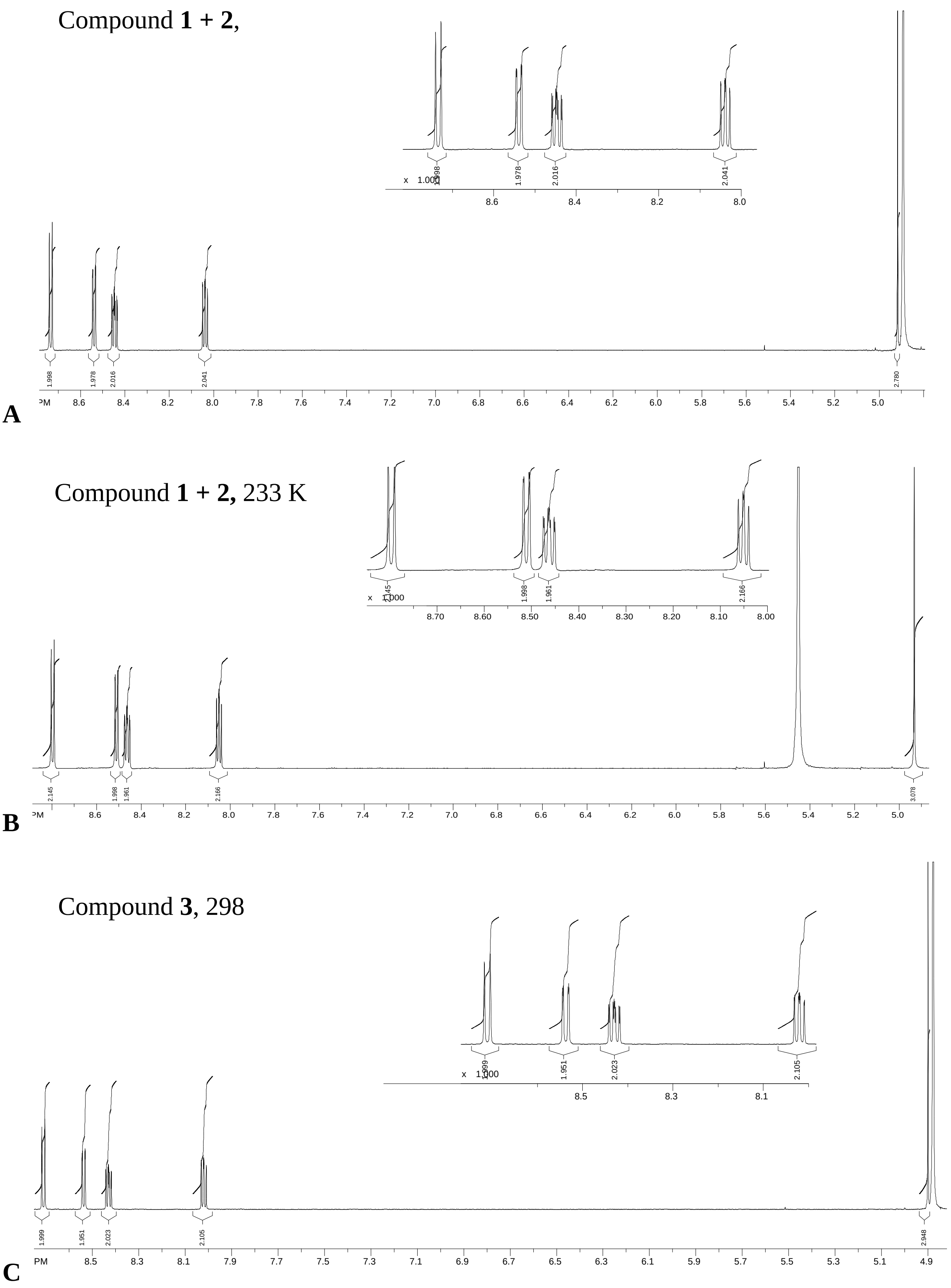

Fig. S2 ^{1}H NMR spectra recorded for compounds **1–3** (Fig. 1, Fig. S2) in methanol-d$_4$. **A** – Mixture of crystals of **1** and **2** at 298 K; **B** – Mixture of crystals of **1** and **2** at 233 K; **C** – Crystals of **3** at 298 K. For details, see Experimental section.

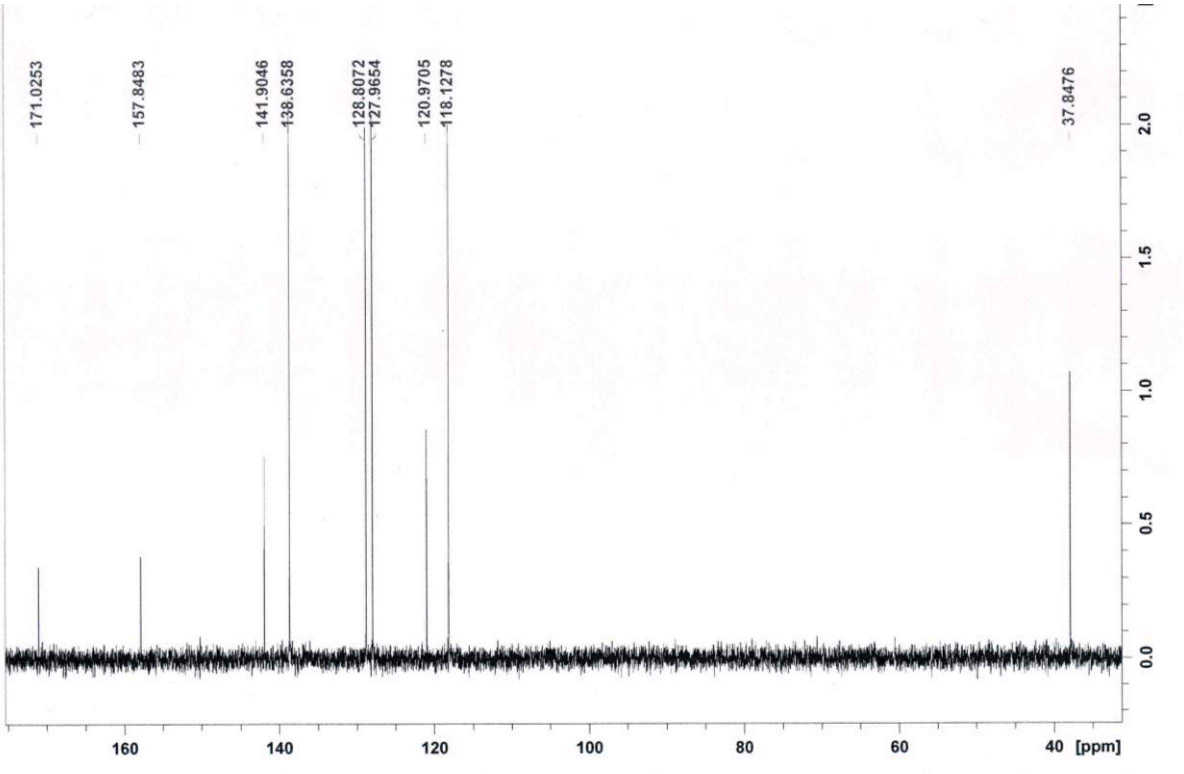

Fig. S3 ^{13}C NMR spectra recorded for compound **3** in D_2O at 298 K. For details see Experimental section.

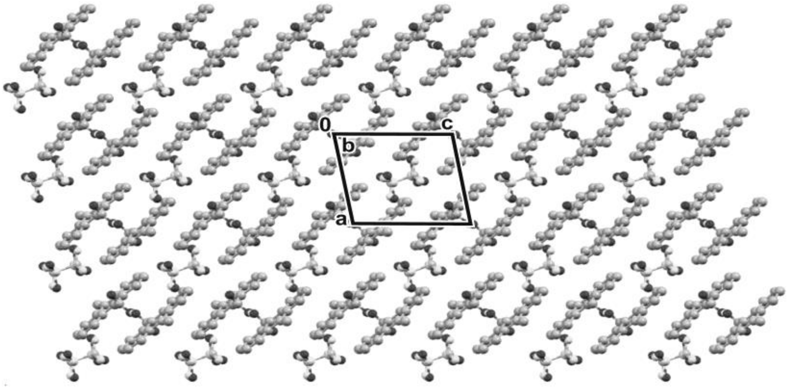

Fig. S4 The crystal packing of **1** viewed along [001] direction (H atoms have been omitted).

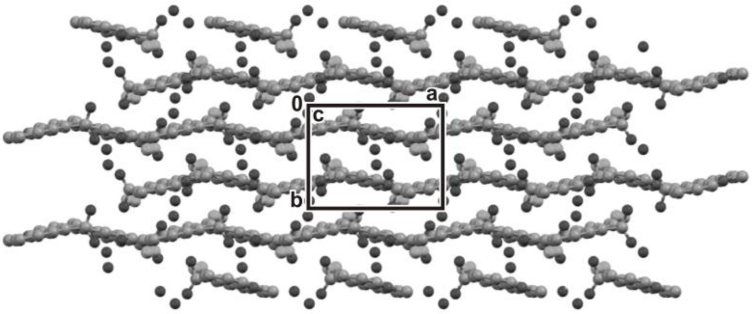

Fig. S5 The crystal packing of **2** viewed along [001] direction (H atoms have been omitted).

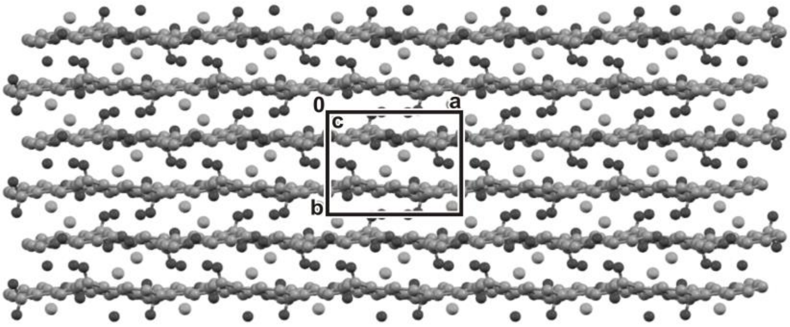

Fig. S6 The crystal packing of **3** viewed along [010] direction (H atoms have been omitted).

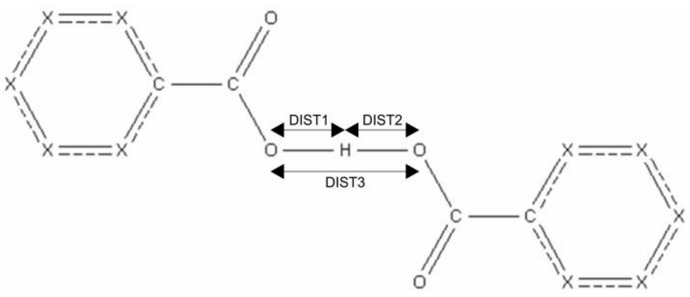

Fig. S7 The geometrical query used for search in the *Cambridge Structural Database*, Version 5.32 (X denotes any atom and DIST1, DIST2 and DIST3 – defined geometric parameters).

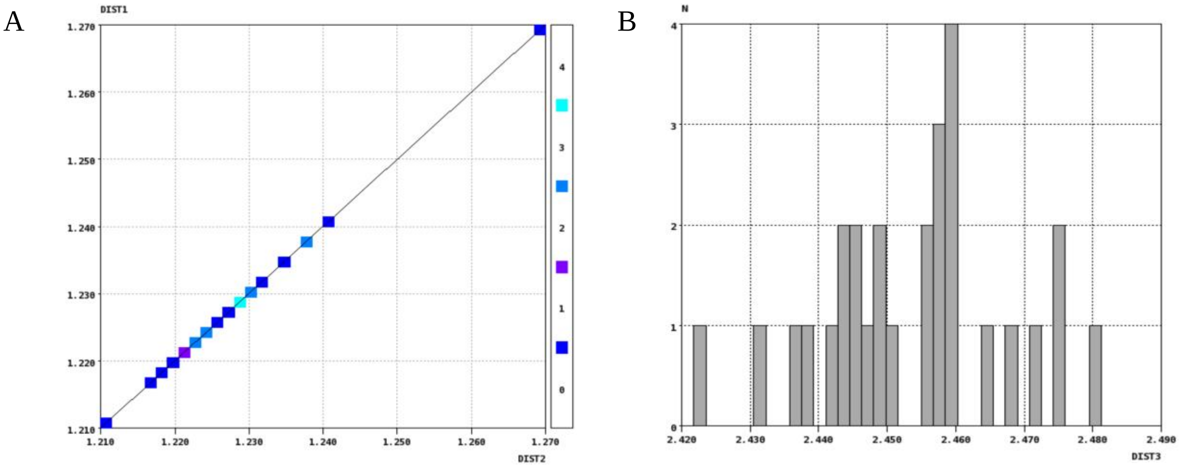

Fig. S8 The data extracted from the CSD Database concerning structural fragments A – The scatterogram correlating O–H···O hydrogen bonds (DIST1 and DIST2) retrieved from 23 examples of homoconjugated cations of aromatic carboxylic systems. B – The histogram showing the distribution of the O···O distance in the O–H···O hydrogen bond occurring in homoconjugated cations of aromatic carboxylic systems found in the CSD Database (mean value: 2.453 Å).

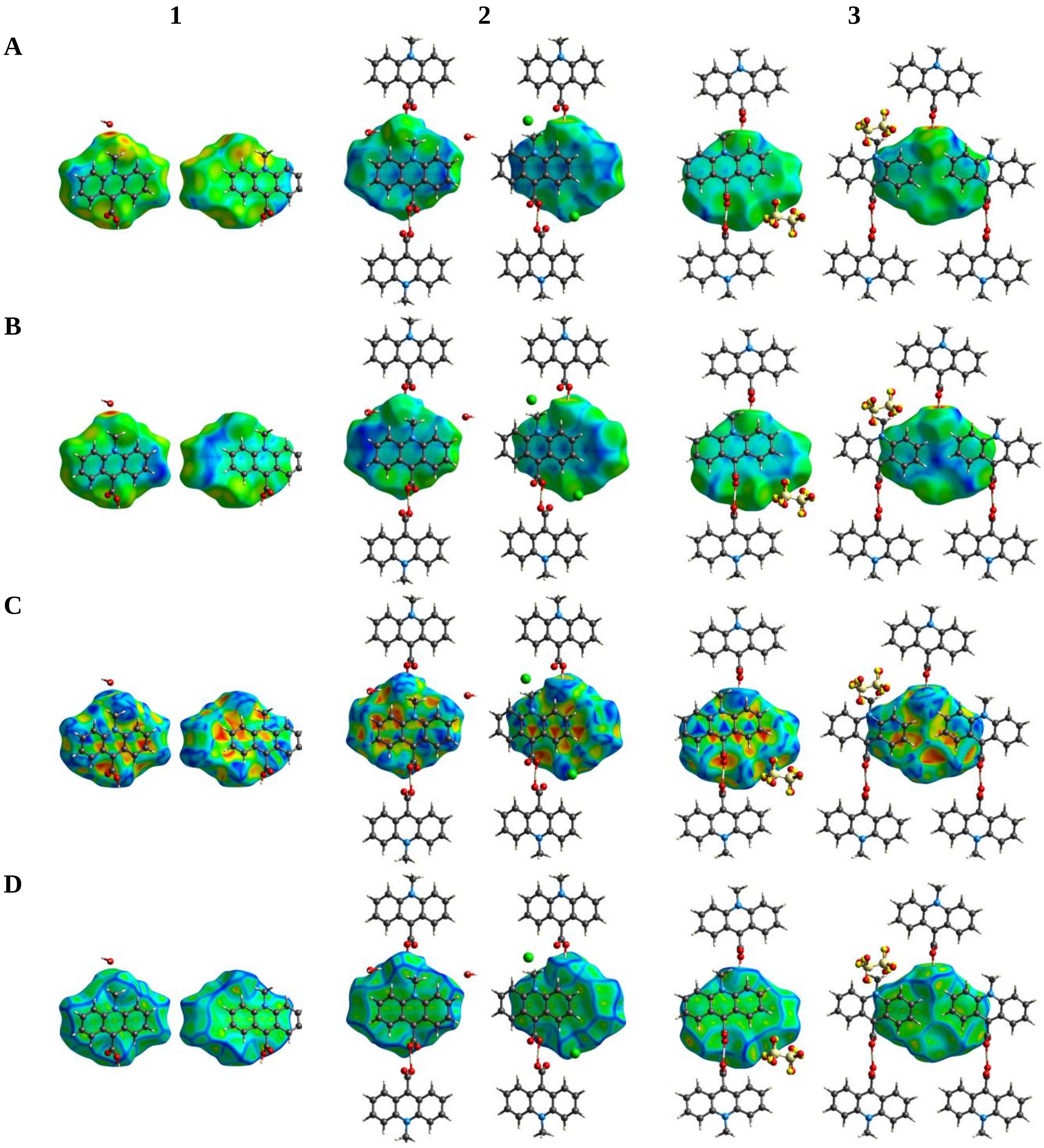

Fig. S9 The Hirshfeld surfaces (front left) and reverse surfaces (right views) representing: **A** – the distance external to the surface (d_e); **B** – the distance internal to the surface (d_i); **C** – the shape-index and D – curvedness together with selected molecules from the surroundings of 9-carboxy-10-methylacridinium (CMA) moieties.

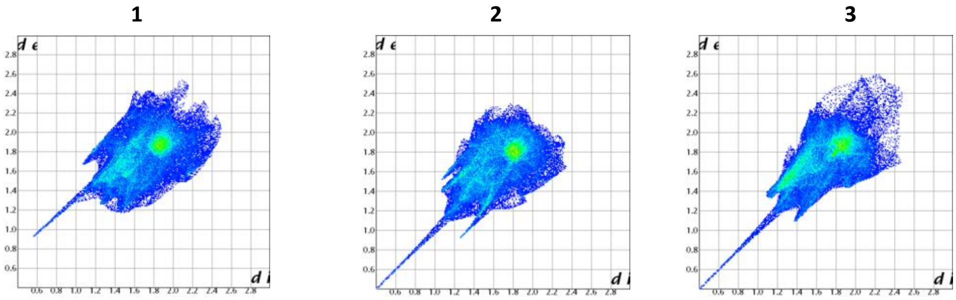

Fig. S10 Comparison of full fingerprint plots of 9-carboxy-10-methylacridinium (CMA) moieties involved in the crystalline compounds investigated (**1**–**3**, Fig. 1).

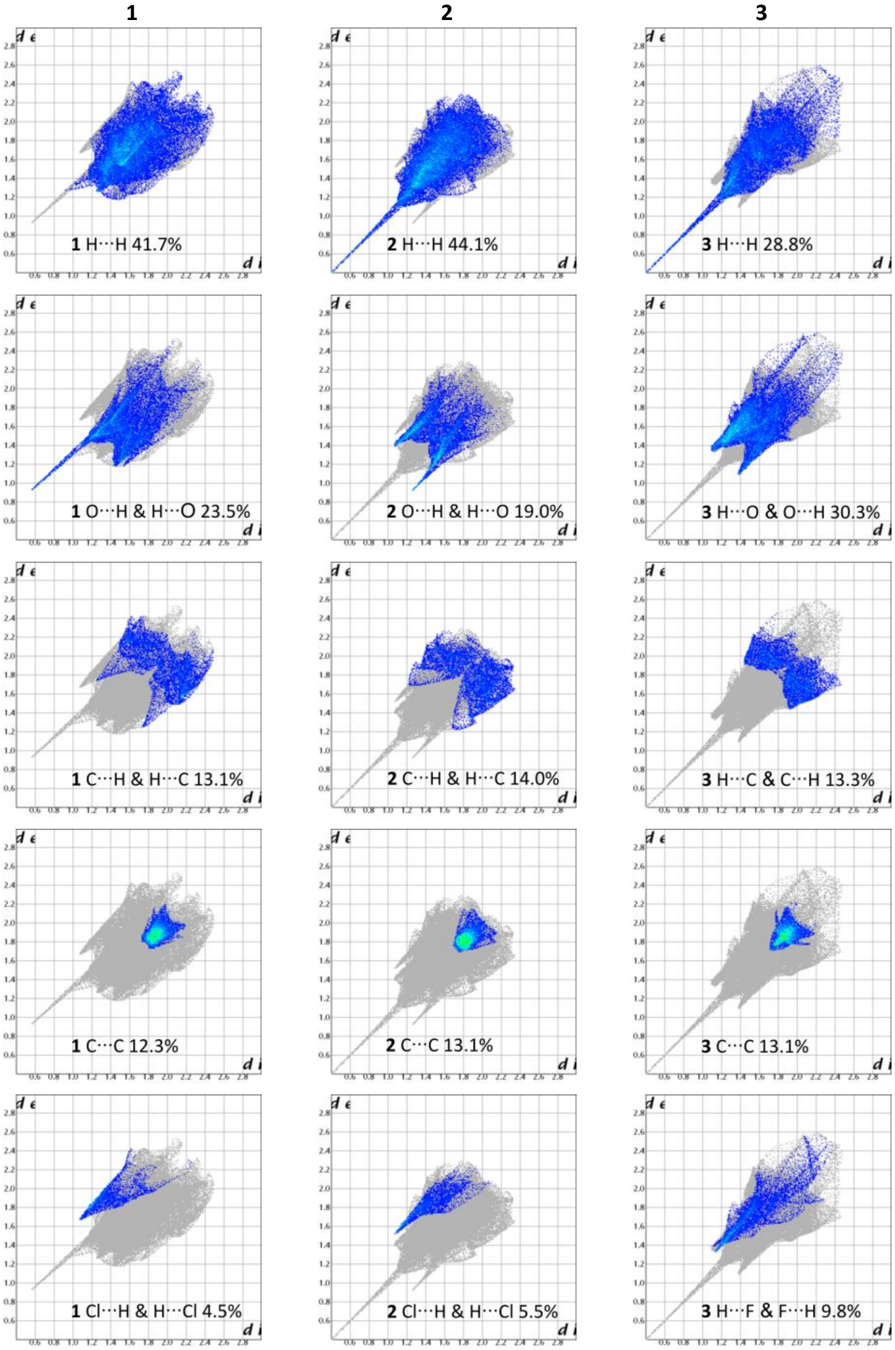

Fig. S11 Fingerprint plots for 9-carboxy-10-methylacridinium (CMA) moieties involved in crystalline compounds investigated (**1**–**3**, Fig. 1), broken down into the contributions arisen from specific pairs of atoms.

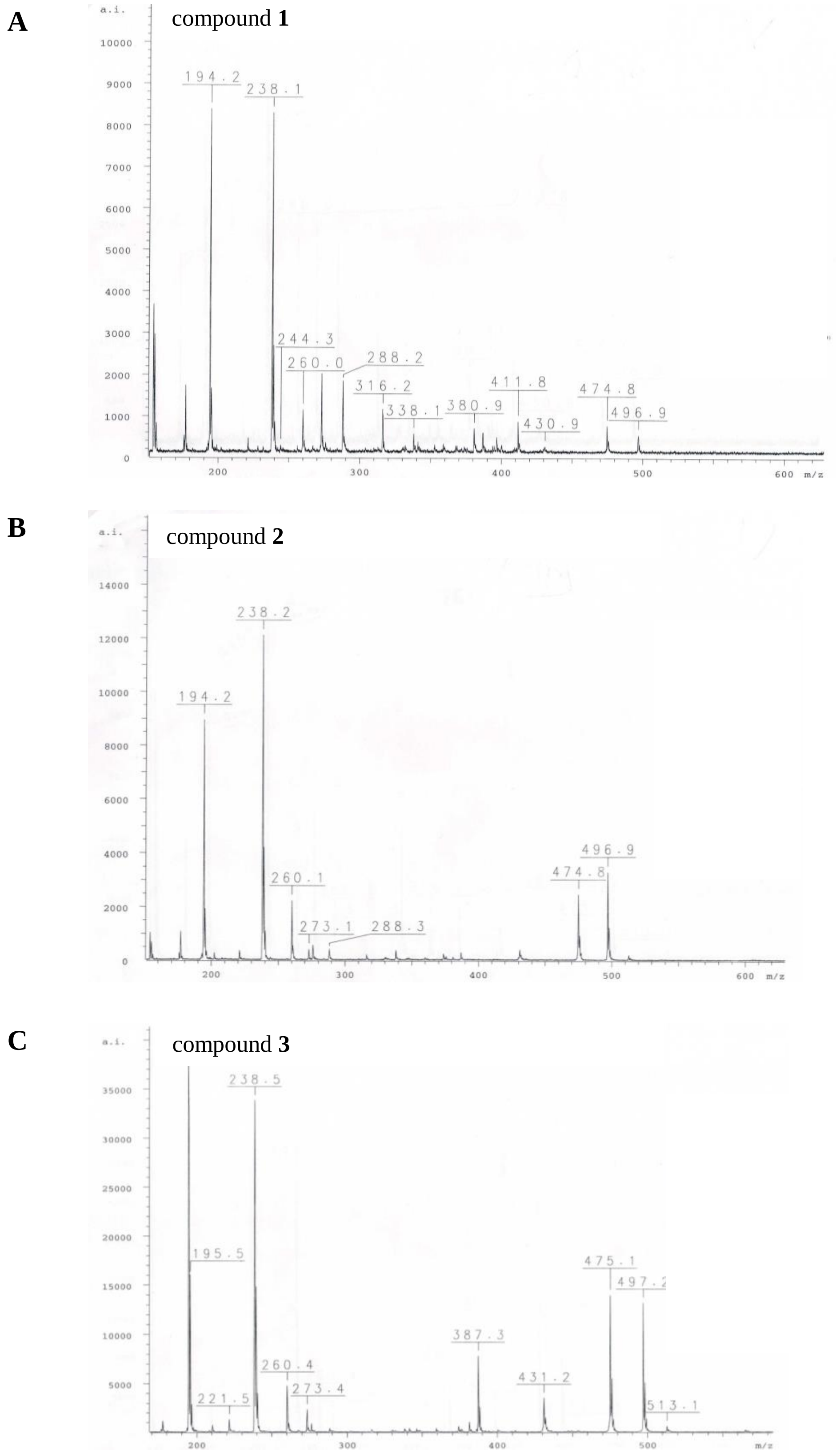

Fig. S12 MALDI-TOF mass spectra for compounds **1–3** dissolved in aqueous matrix **A**: crystals of **1**; **B**: crystals of **2**; **C**: crystals of **3**. See also Table S2 above. For details see Experimental section.

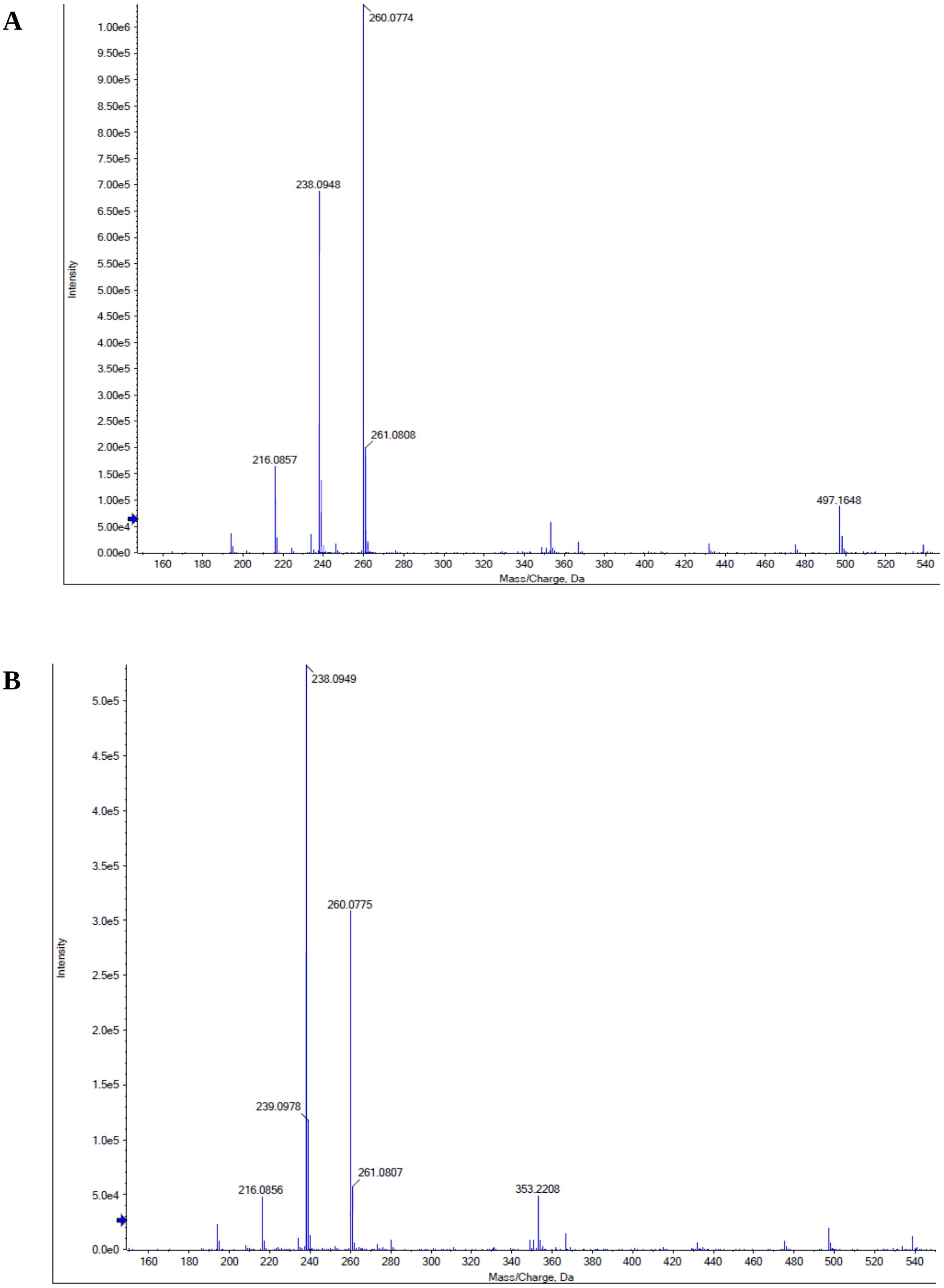
A
Intensity
Mass/Charge, Da
260.0774
238.0948
261.0808
216.0857
497.1648
1.00e6
9.50e5
9.00e5
8.50e5
8.00e5
7.50e5
7.00e5
6.50e5
6.00e5
5.50e5
5.00e5
4.50e5
4.00e5
3.50e5
3.00e5
2.50e5
2.00e5
1.50e5
1.00e5
5.00e4
0.00e0
160
180
200
220
240
260
280
300
320
340
360
380
400
420
440
460
480
500
520
540
B
Intensity
Mass/Charge, Da
238.0949
260.0775
239.0978
261.0807
216.0856
353.2208
5.0e5
4.5e5
4.0e5
3.5e5
3.0e5
2.5e5
2.0e5
1.5e5
1.0e5
5.0e4
0.0e0
160
180
200
220
240
260
280
300
320
340
360
380
400
420
440
460
480
500
520
540

compound **1**

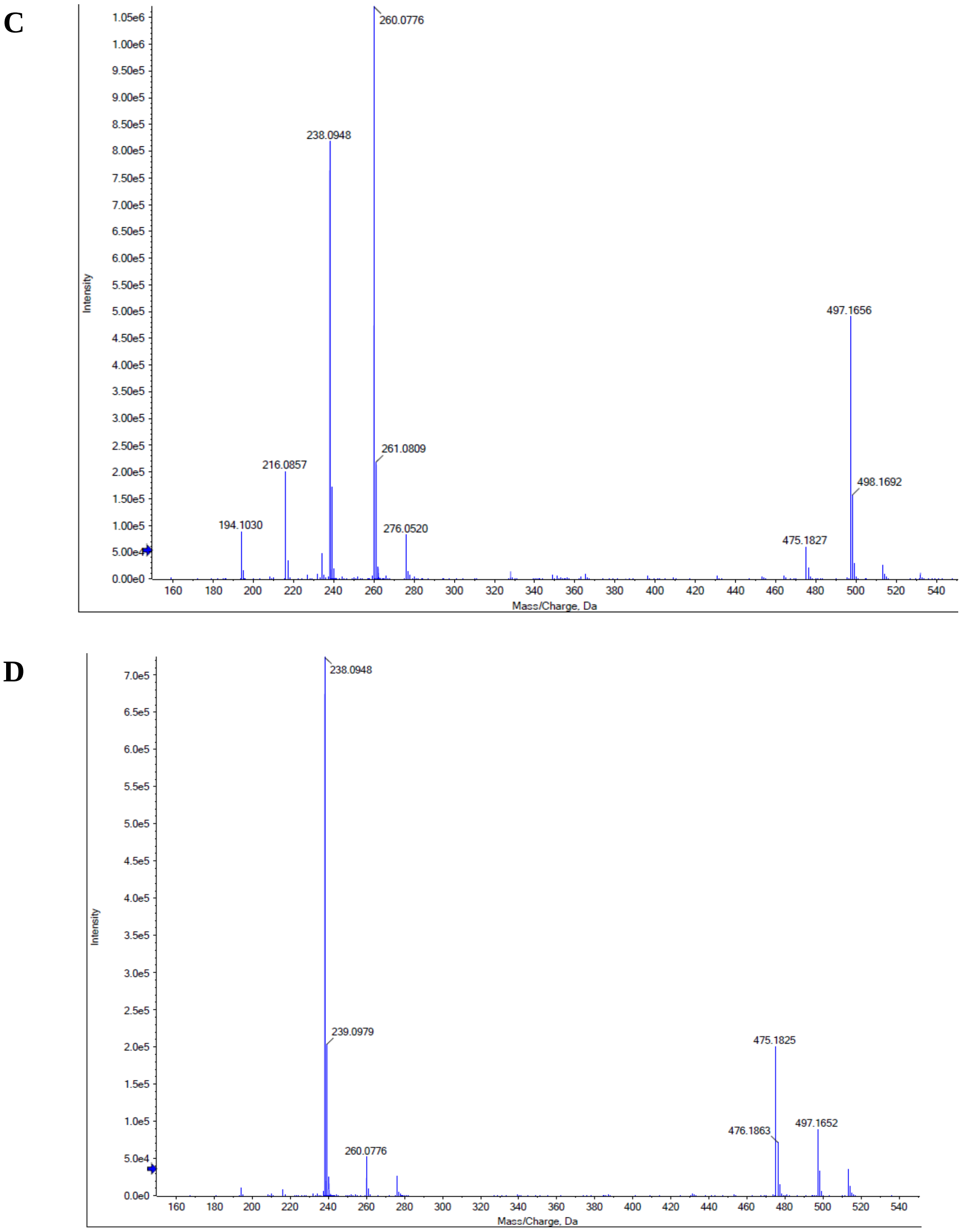

compound **3**

Fig. S13 ESI-QTOF MS spectra for compounds **1** and **3** dissolved in UP water. **A**: compound **1**, mass spectrum taken at the beginning of the chromatographic signal (UPLC) related to 9-carboxy-10-metyloacridinium acid (CMA).

B: compound **1**, mass spectrum taken at the end of the chromatographic signal (UPLC) related to 9-carboxy-10-metyloacridinium acid (CMA).

C: compound **3**, mass spectrum taken at the beginning of the chromatographic signal (UPLC) related to 9-carboxy-10-metyloacridinium acid (CMA).

D: compound **3**, mass spectrum taken at the end of the chromatographic signal (UPLC) related to 9-carboxy-10-metyloacridinium acid (CMA).

For the names of characteristic cationic fragments see Table S2 (above). For details see Experimental section.

A

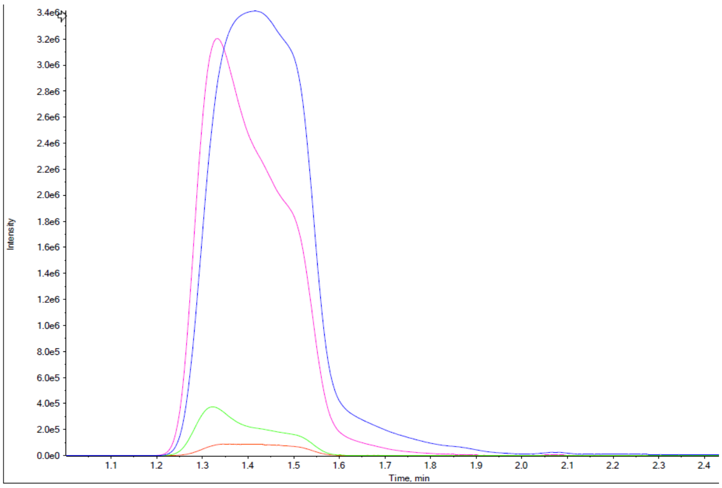

compound **1**

B

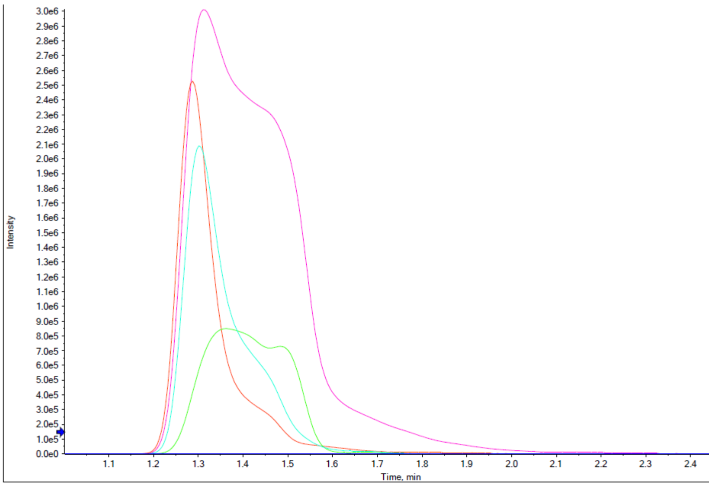

compound **3**

Figure S14. A: The population of various monocations in compound **1**, assessed under UPLC coupled with ESI-QTOF MS experiments. Blue line: m/z ~ 238, pink line: m/z ~ 260, red line: m/z ~ 475, green line: m/z ~ 497.

B: The population of various monocations in compound **3**, assessed under UPLC coupled with ESI-QTOF MS experiments. Pink line: m/z ~ 238, red line: m/z ~ 260, green line: m/z ~ 475, light blue line: m/z ~ 497.

For the names of characteristic cationic fragments see Table S2 (above). For experimental details see text below.

Comments for ESI-QTOF experiments (Figs S13 and S14)

To support MALDI-TOF experiments, we also recorded the mass spectra for **1** and **3** (dissolved in UP water), employing a high-resolution ESI-QTOF mass spectrometer (TripleTOF™ 5600$^+$, AB SCIEX, Canada), coupled with UPLC system (Nexera X2, Shimadzu Co., mobile phase: 0.1% HCO_2H_{aq} at the flow rate of 0.4 ml min^{-1}; stationary phase: Kinetex 2.6µ C18, 100Å column, Phenomenex). The MS operation parameters were as follows: the spray voltage (ISVF) was 5.5 kV, the pressure of nebulizer gas (GS1) and the heating gas (GS2) (N_2) was set at 25 and 30 psi, respectively, the curtain gas pressure (CUR) was equal to 30 psi and the source temperature was 573 K. Declustering potential (DP) was set at 120 V and the collision energy parameter (CE) was set at 9.

The experiments fully confirmed the existence of equilibrium between the monomeric and homoconjugated forms of 9-carboxy-10-metyloacridinium (CMA) monocations, eventually with the participation of the complexes of the above-mentioned forms with sodium or potassium cations (typically observed when using MS techniques). The results allowed to conclude, that the ratio among the above-mentioned forms depends, inter alia, on the time point of the chromatographic signal, at which the mass spectrum was registered. The representative mass spectra are presented in Fig. S13. Generally speaking, the signal intensities clearly indicate, that overall content of the homoconjugated forms is higher in the case of **3** than in the case of **1**, which is consistent with the results obtained with the aim of MALDI-TOF MS (Table S3). In the case of compound **1**, at the beginning of the corresponding chromatographic signal, the monocations complexed with sodium prevail over the native monocations – both in monomeric (m/z ~ 260) as well as in homoconjugated forms (m/z ~ 497). The analyte undergoes desalting process with time and the MS analysis at the end of the chromatographic signal disclose an opposite relationship – the native monocations dominate over the sodium complexes, both in the case of monomeric (m/z ~ 238) and homoconjugated (m/z ~ 475) forms. A similar patterns were observed for the triflate salt (**3**). On the basis of the obtained results, the graphs presenting population of the above-discussed forms vs. chromatography retention time of the main signal were generated and they are presented in Fig. S14. The graphs reflect population of the individual monocationic forms included in **1** and **3** under the applied experimental conditions.

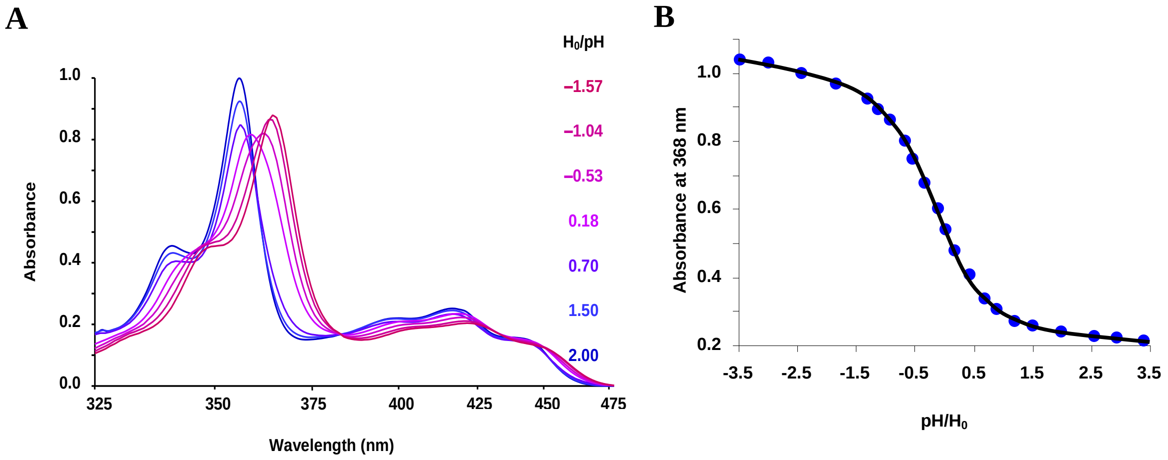

Fig. S15 Spectrophotometric determination of ionization constant (pK_a), characterizing proteolytic equilibrium between zwitterionic and monocationic forms of **1** in H_2O/CH_3CH_3OH system (9/1 v/v). **A**: UV-Vis absorption spectra of **1** in environments of various acidity. **B**: The exemplary UV-Vis titration curve used for calculations of pK_a. For details see the Experimental section.

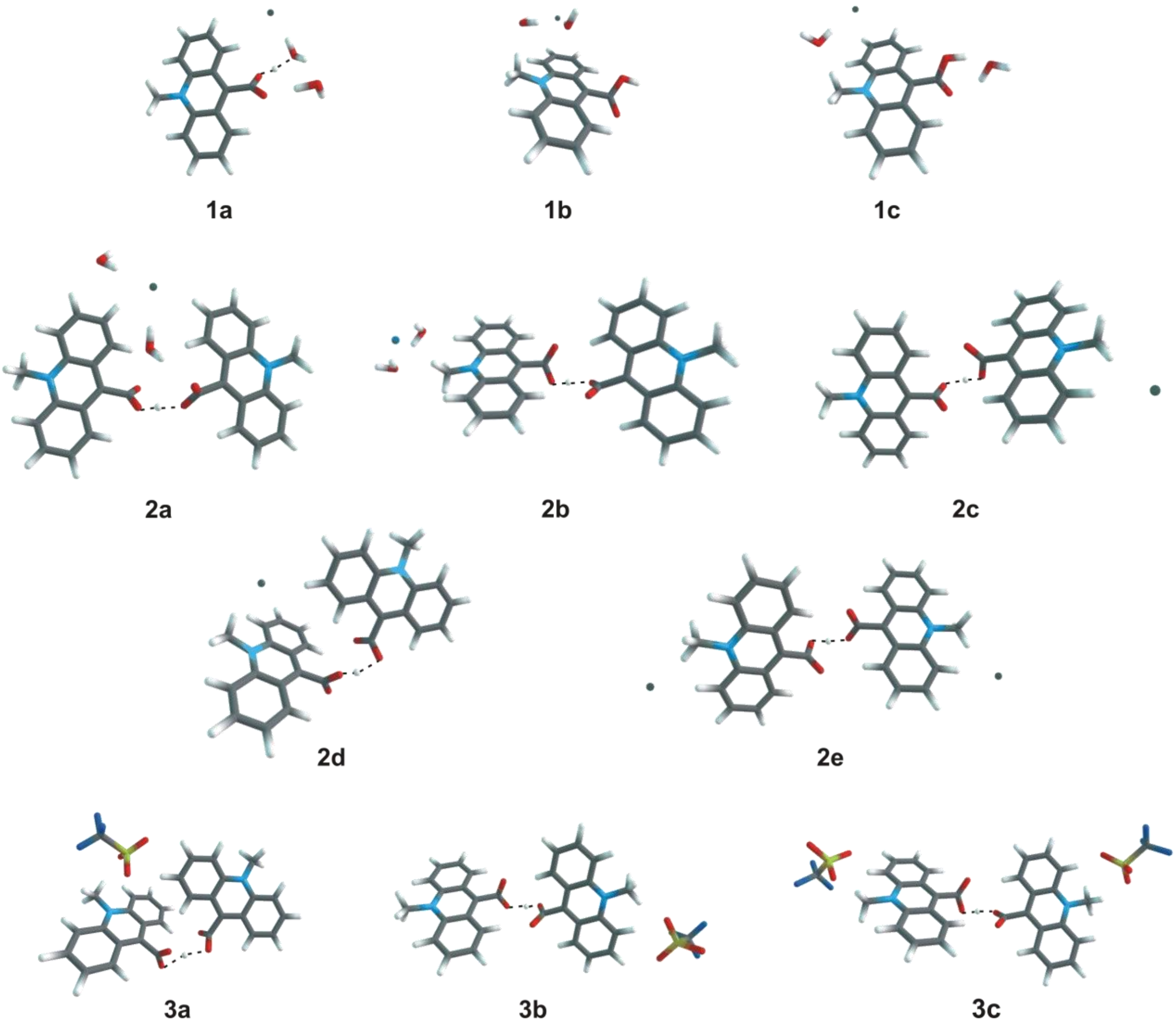

1a 1b 1c

2a 2b 2c

2d 2e

3a 3b 3c

Fig. S16 DFT-predicted gas phase intermolecular complexes formed of 9-carboxy-10-methylacridinium (CMA)-based cations and: (*i*) chloride anions with the participation of water molecules (monocationic forms **1a**–**1c**), (*ii*) chloride anions with the participation of water molecules (homoconjugated forms **2a** and **2b**) and chloride anions (homoconjugated forms **2c**–**2d**) and (*iii*) trifluoromethanesulfonate anions (homoconjugated forms **3a**–**3c**). For details see Experimental section.